Eur. Phys. J. D (2014)
DOI: 10.1140/epjd/e2014-40838-7

THE EUROPEAN PHYSICAL JOURNAL D

Regular Article

Influence of metal ion complexation on the metastable fragmentation of DNA hexamers*

Andreas Piekarczyk[1], Ilko Bald[1,2,3,a], Helga D. Flosadóttir[1], Benedikt Ómarsson[1], Anne Lafosse[4], and Oddur Ingólfsson[1,b]

[1] Science Institute, Department of Chemistry, University of Iceland, Dunhagi 3, 107 Reykjavík, Iceland
[2] Institute of Chemistry – Physical Chemistry, University of Potsdam, 14476 Potsdam, Germany
[3] BAM Federal Institute of Materials Research and Testing, 12205 Berlin, Germany
[4] Univ. Paris-Sud, Institut des Sciences Moléculaires d'Orsay (ISMO), UMR 8214, 91405 Orsay, France

Received 29 December 2013 / Received in final form 15 April 2014
Published online (Inserted Later) – © EDP Sciences, Società Italiana di Fisica, Springer-Verlag 2014

Abstract. Here, we study the metastable decay of 5′-d(TTGCTT) in the presence of 0–6 alkaline metal ions (Li^+, Na^+, K^+, Rb^+) and 0−3 alkaline earth metal ions (Mg^{2+} and Ca^{2+}), which replace the corresponding number of protons in the oligonucleotide. We find that all ions studied here stabilize the oligonucleotide with respect to simple 3′-C–O backbone cleavage, but at the same time these metal ions promote a central oligonucleotide deletion accompanied by a concomitant recombination of the terminal d(TT) groups. We find that the quenching of the 3′-C–O backbone cleavage is not ion specific, since it is due to the removal of the phosphate protons upon replacement with the respective metal ions. The central nucleotide deletion competes with the 3′-C–O backbone cleavage channels and is thus promoted through the replacement of the exchangeable protons against metal ions. However, with increasing positive charge density of the metal ions the yield of the central nucleotide deletion further increases. We attribute this effect to the necessity of sufficient proximity of the terminal d(TT) group to allow for their recombination on this reaction path. Hence, the formation of a reactive conformer is mediated by the metal ions.

1 Introduction

The role of cations in stabilizing DNA and RNA structures, as well as their role in the respective reaction kinetics and catalytic activity of these biologically essential macromolecules is currently a very active research field [1]. The most important cations in biological media are different polyamines, the monovalent alkaline metal ions Na^+ and K^+ and the bivalent alkaline earth metal ions Mg^{2+} and Ca^{2+}. In solution, the solvated metal ions can bind unspecifically with the phosphate groups through diffuse electrostatic interactions and stabilize the DNA through shielding of the abundant excess charge of a DNA strand. The metal ions can, however, also bind sequence specifically to the DNA or RNA strands, stabilizing certain configurations and influencing the overall reactivity of the respective macromolecules. Examples of such specific binding to DNA molecules are the increased Na^+ concentration at the ApT site of the minor groove of the Dickerson-Drew dodecamer [2–4], and the role of cations in the stabilization of the A-, B- and Z-DNA [1]. Furthermore, in RNA particular structural motives, such as loop E motives and AA platforms have been correlated with specific metal ions. In the former case these are Mg^{2+} ions [5–7] and in the latter case K^+ ions [8]. Furthermore, the bivalent cation Mg^{2+} is found to be critical for the formation/stabilization of certain helical junctions [9] and the monovalent cations Na^+ and K^+ are found to be critical in stabilizing different conformers of guanine quadruplexes [10,11]. The screening of the negative charges of the DNA backbone by mono- or divalent cations is also exploited to fabricate dense artificial DNA origami nanostructures [12] and to electrostatically anchor them onto a substrate, e.g., to study sequence-specific radiation induced processes in DNA at the single-molecule level [13].

Until fairly recently the studies of secondary and tertiary structures of native DNA and RNA components and their metal adducts were limited to solution studies or crystallographic examination. In the meanwhile, however, electro spray ionization (ESI) and matrix assisted laser desorption/ionization (MALDI) mass spectrometry have made gas phase studies of quite large DNA and RNA components feasible. In many cases such studies, performed on the isolated molecular species, provide detailed

* Contribution to the Topical Issue "Nano-scale Insights into Ion-beam Cancer Therapy", edited by Andrey V. Solov'yov, Nigel Mason, Paulo Limão-Vieira and Malgorzata Smialek-Telega.

[a] e-mail: ilko.bald@uni-potsdam.de
[b] e-mail: odduring@hi.is

information on the mechanisms of the unimolecular reactivity of these species. However, in the absence of the shielding effect of solvent molecules, secondary and tertiary DNA and RNA structures obtainable in solutions will not necessarily prevail in the gas phase. A number of studies on double stranded oligonucleotides (ONT) have shown that the double strands are conserved in the gas phase and strong indications exist that Watson-Crick base pairing is at least partly preserved [14–16]. Furthermore, through the recent combination of ESI with ion mobility (IM) measurements, it was shown that ONT ions generated in ESI, can at least partly maintain their helical solution structure in the gas phase [14]. Also, in mass spectrometric studies, guanine rich sequences have been shown to aggregate to quadruplexes in the gas phase [17,18] and ESI/IM measurements in combination with MD calculations show strong indications that these maintain their solution structure in the gas phase (at least for the duration of these experiments (1 ms)) [14].

In previous work, we have studied the influence of sodium ions on the stability of hexamer (and octamer) ONTs of the general sequence 5′-d(TTXYTT) with X ≠ Y = A, G or C [19–23]. Hence, two central high PA base nucleotides are surrounded by terminal, more stable d(TT) chains (d(TTT) for the octamers). In these studies it was established that replacing the exchangeable protons against sodium ions stabilizes the ONTs by gradually quenching the 3′-C–O bond cleavage generally observed in PSD of protonated ONTs. These fragmentation channels were attributed to an initial loss of a high PA base in the 3rd or 4th position, respectively, followed by a proton transfer from the central phosphate group to the second high PA base and subsequent cleavage of either the third (w_3) or fourth (a_4 – B_4) 3′-C–O bond (see Figs. 1a and 1b). However, in addition to this stabilization effect it was found that replacement of the exchangeable protons against sodium ions also gradually opens up a new, intriguing fragmentation channel. This channel constitutes a central nucleotide deletion and a recombination of the terminal fragments. The extend of this channel was found to increase with increasing number of protons exchanged against sodium ions up to 5 sodium ions, but to be abruptly turned off when the 6th proton was exchanged against a sodium ion. In these studies, no qualitative difference was found for different central bases as long as these were the high PA bases A, G or C, but the extent of fragmentation through the w_3 and a_4 – B_4 channels was found to be critically dependent on the proton affinity of the central bases. Furthermore, when the higher PA base was in the 3rd position the w_3 channel dominated, but the a_4 – B_4 channel dominated when the higher PA base was in the 4th position.

In the current study we extend this work to encompass the alkaline metal ions Li^+, Na^+, K^+ and Rb^+, as well as the alkaline earth metals Mg^{2+} and Ca^{2+}. The sequences 5′-d(TTGCTT) and 5′-d(TTCATT) were considered, but as these show very similar behavior we limit our discussion here to 5′-d(TTGCTT) as an illustrative example. In particular, we seek to de-convolute the effect simply brought by through the removal of the exchangeable protons and the effects brought by through the influence of the metal ions. While the first is independent of the properties of metal ions the latter is expected to depend critically on these. Mainly we expect the radius of these ions, their positive charge density and their coordination to play a role. While the coordination is expected to be clearly different for the alkaline and alkaline earth ions, the radius of the ion within each group increases gradually with increasing atomic number: Li^+ (0.59−0.92 Å), Na^+ (0.99−1.39 Å), K^+ (1.51−1.78 Å), Rb^+ (1.52−1.83 Å), Mg^{2+} (0.71−1.03 Å) and Ca^{2+} (1.00−1.34 Å) [24].

2 Experiment

The experimental setup and the measurement procedures have previously been described in detail [23]. In brief, the metastable decay measurements were carried out with a commercial MALDI time of flight mass spectrometer (TOF-MS); REFLEX IV (Bruker Daltonics, Bremen, Germany) that is operated in post-source decay (PSD) mode. The REFLEX IV is a reflectron type UV-MALDI-TOF equipped with a 400 μJ/pulse N_2-laser operating at 1−10 Hz and 337 nm. The experiments were performed in positive ion, pulsed delayed extraction mode with 400 ns delay time. The total acceleration voltage was 25 kV resulting in about 30 μs flight time through the field free linear region of the TOF-MS. Protonated parent ions are mass selected with an ion gate placed about 75 cm downstream from the acceleration region. The width of the mass gate was set to be ±3 u when measuring lithium adducts and ±5 u when measuring the sodium adducts, but was set to ±10 u in all other experiments. After the linear flight, the ions were mass analyzed with the reflectron and detected on a double micro-channel plate detector. The reflectron voltage was stepped down in seven segments to assure for observation of all fragment masses from the precursor mass, down to $m/z = 600$. Each segment is the sum of 500 laser shots and is recorded by using the FlexControl™ software provided by the manufacturer. The segments are combined and calibrated to create one PSD mass spectra, using the FlexAnalysis™ software, also provided by the manufacturer. In all experiments, the laser power was kept about 10% above the detection threshold of the respective molecular ions. Mass accuracy was verified by comparing the measured mass of the precursor and that of the w_2 and w_3 fragments (nomenclature by McLuckey et al. [25]) with the calculated masses.

Sample preparation with sodium chloride was carried out as described previously [22]. In brief, a 0.1 mM ONT solution was mixed with 0.5 μL of 10 mM NaCl solution and mixed with 2 μL of saturated aqueous solution of 2,5-dihydroxybenzoic acid (DHB). The solution was then spotted on a polished stainless steel sample plate and allowed to dry in air. For sample preparation with LiCl, KCl, RbCl, $MgCl_2$ and $CaCl_2$ salts, 2 μL of saturated aqueous solution of 2,5-dihydroxybenzoic acid (DHB), was spotted on a polished stainless steel sample plate and allowed

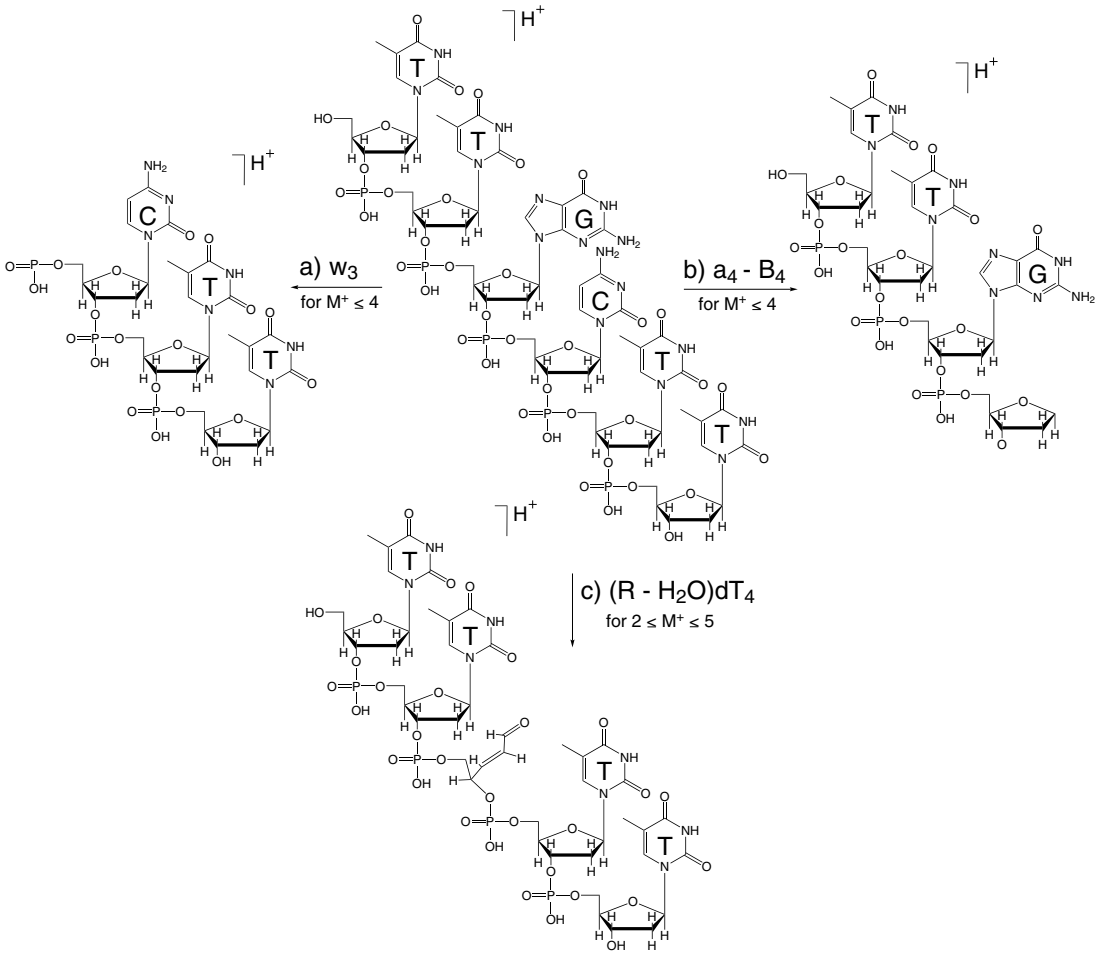

Fig. 1. Reaction scheme showing the molecular structures of 5′-d(TTGCTT) and the most important fragmentation products observed in their metastable decay, namely the w_3 (a), $a_4 - B_4$ (b) and $(R - H_2O)dT_4$ (c), which is due to the central nucleotide deletion. The formation of $(R - H_2O)dT_4$, reaction channel (c), opens up after the exchange of two protons against metal ions and is abruptly "turned off" when six protons are exchanged against metal ions. The backbone cleavage channels (a) and (b), on the other hand, are gradually quenched with increasing number of protons exchanged against sodium ions and are generally close to quantitatively quenched when four protons have been exchanged against metal ions.

to dry in air. Subsequently the respective salt solutions were added to the dried matrix and the spot was allowed to dry again. The reproducibility with different salt concentration was rather poor, but in general post spotting the matrix with 0.5 μL of 10 mM salt solution gave reasonable intensities of parent ions containing 0−6 alkaline metal ions or 0−3 alkaline earth metal ions. After spotting and drying the matrix with the K and Rb salt solutions, 0.5 μL of a 0.1 mM aqueous solution of the ONTs was added and allowed to dry in the air. For preparations of samples containing Li, Mg and Ca salts, on the other hand, 0.5 μL of the 0.1 mM aqueous ONT solutions were desalted prior to spotting by following the ZipTip® (Millipore, Billerica, US) procedure for ONTs and eluted with 0.5 μL of a 50% mixture of isopropanol and deionised water. The ONTs isopropanol/water elute was then spotted on the dried matrix/salt spot and allowed to dry again.

The hexameric ONTs TTGCTT and TTCATT were synthesized and purified in-house as previously described in detail [22].

3 Results and discussion

Figure 1 shows the molecular structure of the parent hexameric oligonucleotide 5′-d(TTGCTT) and the structure of the most important fragmentation products observed in metastable decay. These are the w_3, $a_4 - B_4$ and the fragment resulting from the central nucleotide deletion, which in the following is referred to as $(R - H_2O)dT_4$, where $(R - H_2O)$ signifies the rest of the ribose that remains from the two nucleotides eliminated. The w_3 and $a_4 - B_4$ fragments, channels (a) and (b), are the main 3′-C–O backbone cleavage channels while the $(R - H_2O)dT_4$ fragment formation, channel (c) constitutes a central nucleotide deletion and recombination of the terminal d(TT) groups. The backbone cleavage channels (a) and (b), are gradually quenched with increasing number of protons exchanged against sodium ions and are generally close to quantitatively quenched when four protons have been exchanged against metal ions. The formation of the $(R - H_2O)dT_4$ fragment, on the other hand opens up

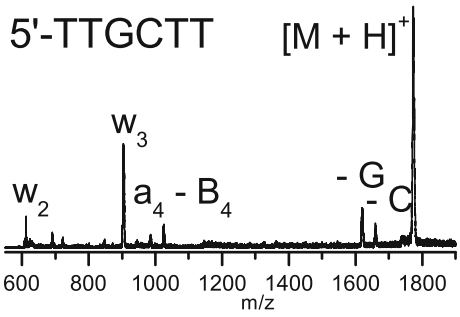

Fig. 2. PSD spectrum of protonated 5′-d(TTGCTT) in the m/z range 550−1900.

after the exchange of two protons against metal ions and is abruptly "turned off" when six protons are exchanged against metal ions.

3.1 Quenching of w_3 and a_4-B_4 fragmentation channels

The PSD spectrum of protonated 5′-d(TTGCTT) is shown in Figure 2. It is characterized by the loss of G and/or C, initiated by protonation of one of these bases, and cleavage of the 3′-C–O bond subsequent to the base eliminating (w_3 and a_4 – B_4). For detailed discussion on the mechanism behind these channels we refer to references [21,22] and literature cited therein. The PA of the DNA nucleobases increases in the order T < A < C < G [26] and correlates directly with their stability in PSD of the protonated ONTs [22]. The loss of these bases, rather than thymine, is thus attributed to their high PA. For 5′-d(TTGCTT) the w_3 fragmentation is the most dominant channel, since the higher PA base (G) is located at the third position. In the case of 5′-d(TTCGTT), on the other hand, (not considered here), the a_4 – B_4 channel dominates [21].

Figure 3 shows PSD spectra of 5′-d(TTGCTT) after exchange of the phosphate protons with 1−6 alkaline ions (Li^+, Na^+, K^+, Rb^+). The spectra are shown in the m/z range covering the w_3 and a_4 – B_4 fragments and the central nucleotide deletion discussed above. Further fragments rooting from different backbone cleavage channels are also visible in the spectra. Most noticeable of these is a fragment that appears 112 mass units below the respective a_4 – B_4 fragments. This fragment, which we attribute to a 5′-P–O bond rupture after the third nucleoside, is most obvious in the traces where protons have been exchanged against potassium or rubidium ions. The backbone cleavage channels all show qualitatively the same trend when protons are exchanged against alkaline or alkaline earth metal ions and we thus limit our discussion to the most pronounced w_3 and a_4 – B_4 channels. Also, in the traces where 3 protons have been exchanged against alkaline ions in the parent molecule, significant satellite peaks due to a fraction of the w_3 contribution that contains only two alkaline metal ions are present. This effect is also visible in the traces where 4 protons have been exchanged against alkaline ions, but to a much lesser extent.

Since the backbone cleavage depends critically on the availability of a phosphate proton, the reaction is gradually quenched when the phosphate protons are replaced by the metal ions. To enable a comparison of the signal intensities between the spectra, the intensity scale is normalized to the sum of the signals representing the precursor ions for the backbone cleavage reactions, i.e., the protonated parent ions MH^+ and the protonated parent ions after loss of G or C ($[MH^+ - G]$ and $[MH^+ - C]$), respectively (M represents the molecular precursor with the respective metals). The PSD spectra shown in Figure 3 demonstrate that the quenching of the backbone cleavage (w_3, a_4 – B_4 fragments) occurs to a similar extent for all alkaline ions. In the presence of four Li^+ or Na^+ ions the quenching of the backbone cleavage is complete, whereas one more ion is required in the case of K^+ and Rb^+. The quenching of these channels is also observed with alkaline earth metal ions, as is shown in Figures 4a and 4b, which display the PSD spectra of protonated 5′-d(TTGCTT) where exchangeable protons have been replaced with the doubly charged ions Mg^{2+} and Ca^{2+}, respectively. The backbone cleavage is in these cases already suppressed by two Ca^{2+} or Mg^{2+} ions, compared to the alkaline metal ions where at least four ions are required for complete quenching of these channels. This is readily understandable as two of these alkaline earth metal ions replace four protons. Hence, the quenching of the w_3 and a_4 – B_4 channels is solely the result of the removal of the exchangeable protons and does not depend on the nature of the metal ions. This is also concordant with the first step in the mechanism behind the formation of these fragments (after the base loss) involving a proton transfer from a neighboring phosphodiester group [22].

3.2 Central nucleotide deletion

Apart from the quenching of the 3′-C–O backbone cleavage the replacement of the exchangeable protons with alkaline or alkaline earth ions induces a remarkable deletion of the two central nucleotides less a dehydrated ribose rest that remains with the charged fragment. This channel gives rise to the formation of the fragment ion $(R - H_2O)dT_4$, which is composed of all the two terminal thymidine units and thus requires a recombination of these. As described previously [21], the loss of the high PA base is the initial step for this reaction. The base loss is then anticipated to be followed by a nucleophilic attack of an adjacent phosphate at the positively charged sugar residue that results from the base loss. This leads to an elimination of the second high PA base as a neutral fragment and a recombination of the terminal d(TT) groups. The initial step in the formation of $(R - H_2O)dT_4$, i.e., the base loss, is thus the same as the initial step leading to the w_3 and a_4 – B_4 fragments. From Figure 3 it can be seen that the formation of $(R - H_2O)dT_4$ apparently starts to be operative in the presence of 1−3 alkaline ions. For Li^+ ions the signal is already discernable when one proton has been replaced, for Na^+ ions when two protons have been replaced, for K^+ when one proton has been replaced and

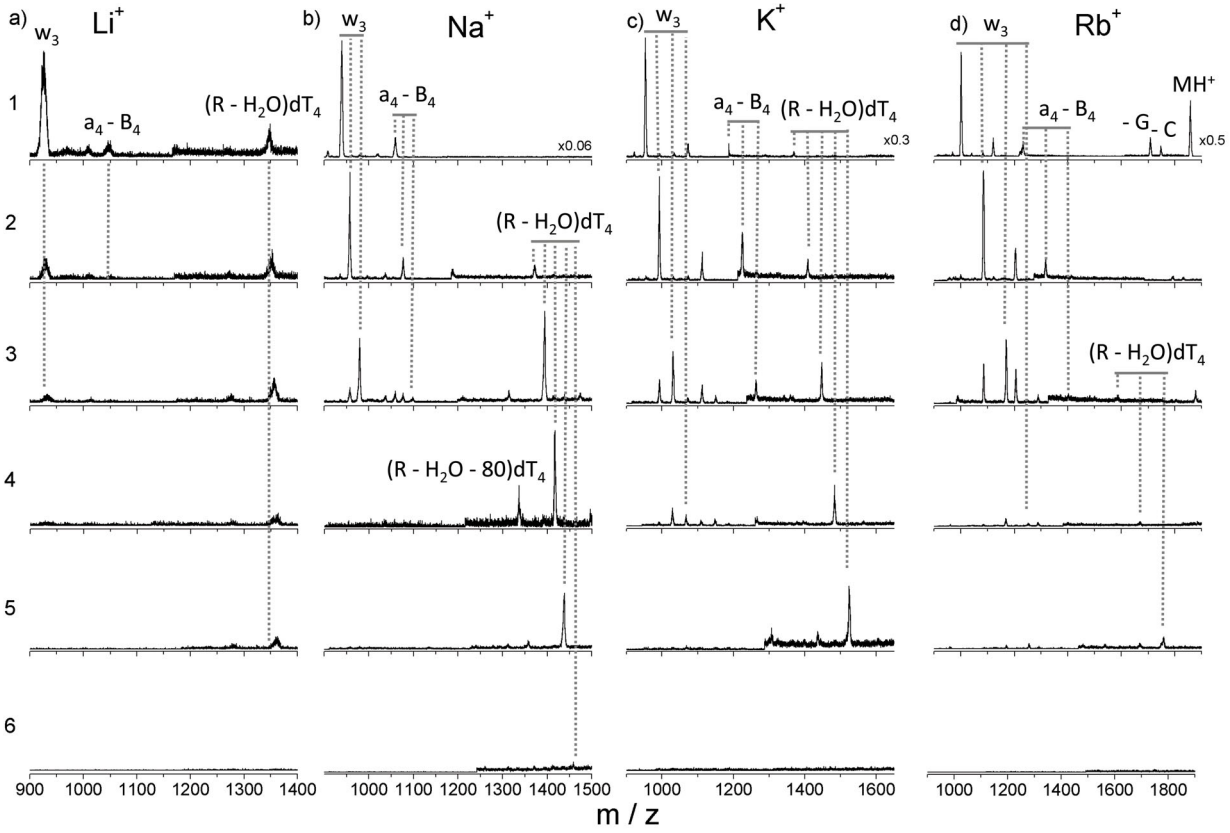

Fig. 3. PSD spectra of protonated 5′-d(TTGCTT) with 1–6 protons exchanged against alkaline metal ions Li^+ (a), Na^+ (b), K^+ (c), and Rb^+ (d). The respective m/z range shown is chosen for convenient comparison of the backbone cleavage (w_3, $a_4 - B_4$) and central nucleotide deletion channels ($(R - H_2O)dT_4$). Intensity scales were normalized to the sum of the intensities recorded for the respective protonated parent ions MH^+, and the $MH^+ - G$ and $MH^+ - C$ base loss peaks.

for Rb^+ when three protons have been replaced. However, due to the gate width of about 6 Da the Li^+ ion coordinated ONTs cannot be unambiguously assigned to a single species and we attribute the occurrence of the $(R - H_2O)dT_4$ fragments in the PSD spectrum with one Li^+ ion to a contribution from the protonated ONT with two Li^+ ions. Similarly we attribute the weak signal of the $(R - H_2O)dT_4$ fragment seen in the PSD spectra for one K^+ to protonated 5′-d(TTGCTT) after exchange of two protons against Na^+, since the presence of Na^+ ions cannot be completely avoided. We are thus confident to state that for Li^+, Na^+ and K^+ two protons must be exchanged against the metal ions to initiate this channel, while three are needed in the case of Rb^+. As described in the experimental section, individual segments of the mass spectra are recorded sequentially. These are however recorded under identical conditions and are composed of 500 individual laser shots each. Thus, while the comparison between different segments is not a strict quantitative measure, it still gives a fair picture of the relative intensity of individual fragments. From the PSD spectra with three alkali ions in Figure 3, it can be seen that the $(R - H_2O)dT_4$ formation is more intense than the w_3 fragmentation for Li^+ and Na^+, but less intense for K^+ and eventually very weak for Rb^+. To visualize this effect more clearly the intensity ratio of the $(R - H_2O)dT_4/w_3$ signals for parent ions with three protons exchanged against alkaline metal ions is plotted in Figure 5. It is clear from this figure (and Fig. 3) that the central nucleotide deletion becomes less favorable with increasing size of the alkaline metal ions, hence, with decreasing positive charge density.

Qualitatively the same behavior is observed in the PSD spectra of the protonated 5′-d(TTGCTT) when the exchangeable protons have been replaced by the bivalent alkaline earth metal ions Mg^{2+} and Ca^{2+} (Fig. 4). In the presence of one of these ions, the intensity of the $(R - H_2O)dT_4$ signals is already higher than the w_3 signals, and it is also clear from Figure 4, that the $(R - H_2O)dT_4$ formation is more efficient in the case of Mg^{2+} than in the case of Ca^{2+}. This, in turn, supports our conclusion above that increasing positive charge density promotes this channel.

Figure 6 compares the PSD spectra obtained for 5′-d(TTGCTT) with four protons exchanged against four Na^+ ions and two Ca^{2+} ions, respectively. In both cases the w_3 fragmentation is completely quenched but the $(R - H_2O)dT_4$ fragment occurs to be less intense in the case of the Ca^{2+} ions when compared with the G/C base loss fragments, proceeding this channel. Na^+ and Ca^{2+} ions possess almost the same ionic radius, but different positive charge density, however, a comparison as given above is not necessarily valid as here we are comparing

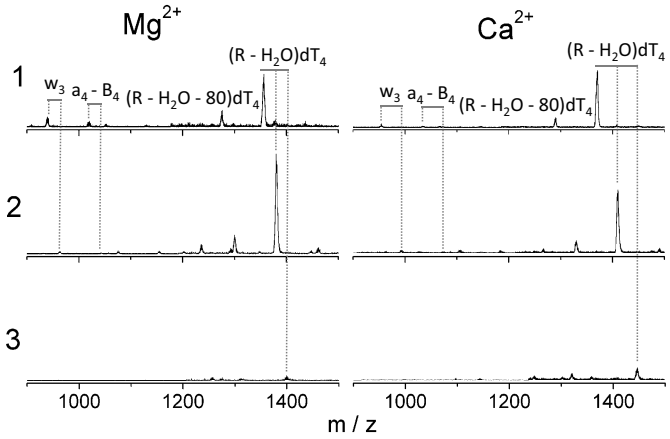

Fig. 4. PSD spectra of protonated 5′-d(TTGCTT) with 2, 4 or 6 protons exchanged against alkaline earth metal ions Mg^{2+} (left panel) and Ca^{2+} (right panel). The respective m/z range shown was chosen for convenient comparison of the w_3, $a_4 - B_4$ and $(R - H_2O)dT_4$ fragmentation channels. Intensity scales were normalized to the sum of the intensities recorded for the protonated parent ions MH^+, and the $MH^+ - G$ and $MH^+ - C$ base loss peaks.

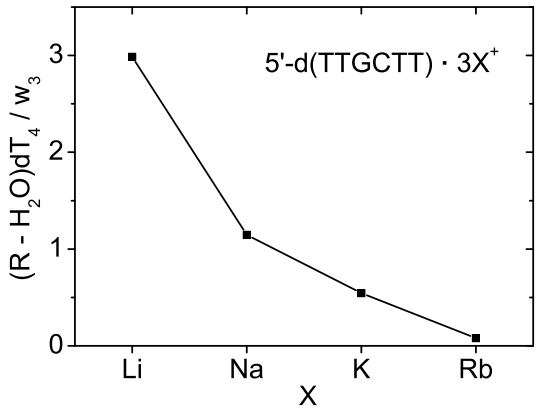

Fig. 5. Plot of the ratio of signal intensities of the $(R - H_2O)dT_4$ fragment to that of the w_3 fragment ($(R - H_2O)dT_4/w_3$) in the presence of three alkaline ions.

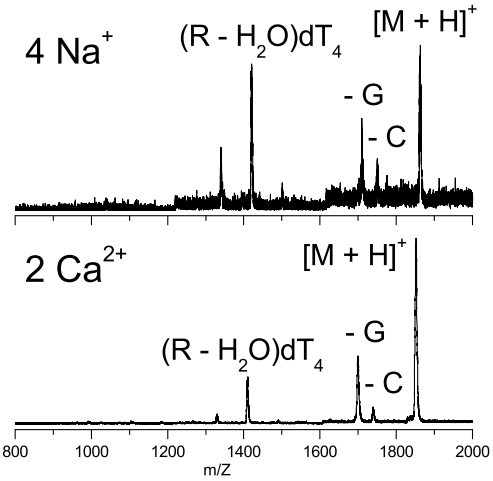

Fig. 6. Comparison of PSD spectra of protonated 5′-d(TTGCTT) with 4 protons exchanged against four sodium ions Na^+ (upper spectrum) and two calcium ions Ca^{2+} (lower spectrum). Intensity normalization was performed as in Figure 2.

the influence of four ions against that of two ions and the coordination is thus very different. Nonetheless, from the comparison of these spectra as well as those shown in Figures 3 and 4 it is clear that the number of exchanged protons is the most important factor determining to which extent the central nucleotide deletion is operative, and that the influence of the positive charge density and the coordination of the respective ions is of less importance.

This is concordant with a picture, in which the backbone cleavage and the central nucleotide deletion are competing channels. Both these channels are initiated through protonation of the highest PA base and subsequent base loss. The backbone cleavage, however, is also critically dependent on the availability of an exchangeable proton at one of the phosphate groups and is thus gradually quenched as these are replaced by metal ions, and is generally close to being quantitatively quenched when four protons have been replaced. This in turn shifts the branching ratio in favor of the $(R - H_2O)dT_4$ formation. This channel, however, is also dependent on the reactive ONT conformation that enables the deletion of the central nucleotides and concomitant recombination of the terminal nucleotides. This reactive conformation is established through coordination to the metal ions and from Figures 3–5 it is clear that this coordination is favored with increasing positive charge density of the ions. This interpretation is further supported by the observation that the $(R - H_2O)dT_4$ is abruptly turned off when the sixth proton is exchanged against a metal ion. Hence, the first five ions replace the protons at the phosphate groups, whereas the sixth charge must be coordinated to the highest PA base. The quenching of the $(R - H_2O)dT_4$ fragment after complexation with six charges can thus be explained by the inhibition of the initial fragmentation step, i.e., the protonation and subsequent elimination of the highest PA base. The weak signals in the case of three Ca^{2+} or Mg^{2+} ions, respectively, is most likely due to a limited coordination of the third ion to both a phosphate group and the central nucleobase.

Finally we note that the minor fragmentation channel $(R - H_2O\text{-}80)dT_4$, that is obviously related to the central deletion, was discussed previously [22], where it was tentatively ascribed to an additional loss of either HPO_3 or C_5H_4O. This fragment is signified in the mass spectra for the sodium, calcium and magnesium ions, where it is most apparent.

4 Conclusion

The present study demonstrates that the substitution of the exchangeable protons with metal ions has a profound effect on the PSD reactivity of protonated ONTs, and that such substitution can both quench reactions and open up

new fragmentation channels. It is also clear that these effects are not restricted to the previously studied Na^+ complexes, but are generally observed in PSD of complexes of the hexamer 5′-d(TTGCTT) with alkaline and alkaline earth metal ions. It is also clear that the main channels, i.e., the backbone cleavage leading to the w_3 and the $a_4 - B_4$ fragments and the central nucleotide deletion leading to the $(R - H_2O)dT_4$ fragment, are critically dependent on the availability of a proton at one of the high PA bases. Hence, both these channels proceed after an initial high PA base loss (see also Refs. [21,22]). The formation of the w_3 and $a_4 - B_4$ fragments through a phosphodiester bond rupture, however, is also critically dependent on the availability of a proton at one of the phosphate groups, as is clear from the gradual quenching of these channels with increasing number of phosphate protons exchanged against metal ions. As the central nucleotide deletion leading to the $(R - H_2O)dT_4$ formation and the backbone cleavage leading to the w_3 and $a_4 - B_4$ fragments are competing channels (after the initial base loss), the sequential quenching of the backbone cleavage through substitution of the phosphate protons by metal cations gradually favors the central nucleotide deletion leading to the $(R - H_2O)dT_4$ formation. The extent of this effect depends merely on the number of removed protons and is thus only dependent on the number of charges carried by the respective cations. However, for the $(R - H_2O)dT_4$ formation, a certain proximity of the recombining terminal d(TT) groups is necessary, hence, the formation of this fragment requires a folding of the ONTs that must be stabilized through the respective cations involved. This effect is, in turn, much more subtle than the simple removal of the phosphate protons and depends on the nature and the coordination of the cations within the respective DNA strands. The fact that both these effects contribute to increasing appearance of the $(R - H_2O)dT_4$ fragment in the mass spectra makes it difficult to entangle the role of the individual cations in enabling the folding required for the $(R - H_2O)dT_4$ formation. Nevertheless, it is clear from the current study that this folding is favored with increasing positive charge density on the cations.

In this context it is worth noting that such folding is a dynamic process that has been associated with T base stacking and was observed for octamers; TTTGCTTT, even in the absence of substituting metal ions [21]. Hence, the higher flexibility of the octamers allows for T base stacking of the terminal groups without any stabilization through metal cations while such stabilization is essential for the more rigid hexamers.

To elucidate further details of the coordination of the different metal ions to the protonated hexameric oligonucleotides and the resulting shape of the metal ion-DNA complexes further investigations will be needed. A promising technique is ion mobility spectrometry, where conformation changes may be elucidated.

This work was supported by the Icelandic Centre for Research (RANNÍS) and by the University of Iceland Research Fund. H.D.F. acknowledges a Ph.D. Grant from the Eimskip University Fund. I.B. acknowledges support through an exchange grant by the European Science Foundation (ESF) program: Electron induced processes at the molecular level (EIPAM), and support by the Deutsche Forschungsgemeinschaft (DFG) and the University of Potsdam. This work was conducted within the framework of the COST Actions MP1002 (Nano-IBCT).

References

1. J. Müller, Metallomics **2**, 318 (2010)
2. M.A. Young, B. Jayaram, D.L. Beveridge, J. Am. Chem. Soc. **119**, 59 (1997)
3. X.Q. Shui, L. McFail-Isom, G.G. Hu, L.D. Williams, Biochemistry **37**, 8341 (1998)
4. F.C. Marincola, V.P. Denisov, B. Halle, J. Am. Chem. Soc. **126**, 6739 (2004)
5. N.B. Leontis, P. Ghosh, P.B. Moore, Biochemistry **25**, 7386 (1986)
6. C.C. Correll, B. Freeborn, P.B. Moore, T.A. Steitz, Cell **91**, 705 (1997)
7. M.J. Serra, J.D. Baird, T. Dale, B.L. Fey, K. Retatagos, E. Westhof, RNA **8**, 307 (2002)
8. S. Basu, R.P. Rambo, J. Strauss-Soukup, J.H. Cate, A.R. Ferre-D'Amare, S.A. Strobel, J.A. Doudna, Nat. Struct. Biol. **5**, 986 (1998)
9. D.M.J. Lilley, R.M. Clegg, Ann. Rev. Biophys. Biomol. Struct. **22**, 299 (1993)
10. B. Lippert, D. Gupta, Dalton Trans. **24**, 4619 (2009)
11. P. Schultze, N.V. Hud, F.W. Smith, J. Feigon, Nucleic Acids Res. **27**, 3018 (1999)
12. P.W.K. Rothemund, Nature **440**, 297 (2006)
13. A. Keller, I. Bald, A. Rotaru, E. Cauet, K.V. Gothelf, F. Besenbacher, ACS Nano **6**, 4392 (2012)
14. J. Gidden, E.S. Baker, A. Ferzoco, M.T. Bowers, Int. J. Mass Spectrom. **240**, 183 (2005)
15. V. Gabelica, E. De Pauw, J. Mass Spectrom. **36**, 397 (2001)
16. P.D. Schnier, J.S. Klassen, E.E. Strittmatter, E.R. Williams, J. Am. Chem. Soc. **120**, 9605 (1998)
17. F. Rosu, V. Gabelica, C. Houssier, P. Colson, E. De Pauw, Rapid Commun. Mass Spectrom. **16**, 1729 (2002)
18. D.R. Goodlett, D.G. Camp, C.C. Hardin, M. Corregan, R.D. Smith, Biol. Mass Spectrom. **22**, 181 (1993)
19. H.D. Flosadóttir, B. Omarsson, I. Bald, O. Ingólfsson, Eur. Phys. J. D **66**, (2012)
20. I. Bald, H.D. Flosadóttir, B. Omarsson, O. Ingólfsson, Int. J. Mass Spectrom. **313**, 15 (2012)
21. H.D. Flosadóttir, K. Gislason, S.T. Sigurdsson, O. Ingólfsson, J. Am. Soc. Mass Spectrom. **23**, 690 (2012)
22. H.D. Flosadóttir, M. Stano, O. Ingólfsson, J. Am. Soc. Mass Spectrom. **20**, 689 (2009)
23. M. Stano, H.D. Flosadóttir, O. Ingólfsson, Rapid Commun. Mass Spectrom. **20**, 3498 (2006)
24. R.D. Shannon, Acta Crystallogr. A **32**, 751 (1976)
25. S.A. McLuckey, G.J. Vanberkel, G.L. Glish, J. Am. Soc. Mass Spectrom. **3**, 60 (1992)
26. E.P.L. Hunter, S.G. Lias, J. Phys. Chem. Ref. Data **27**, 413 (1998)